International Journal of Environmental Science and Technology (2020) 17:3397–3410
https://doi.org/10.1007/s13762-020-02719-8

ORIGINAL PAPER

Green approach for the synthesis of ultrafiltration photocatalytic membrane for tannery wastewater: modeling and optimization

Z. Arif[1] · N. K. Sethy[1] · P. K. Mishra[1] · B. Verma[1]

Received: 5 December 2019 / Revised: 7 February 2020 / Accepted: 16 March 2020 / Published online: 18 May 2020

Abstract
A novel polyvinylidene fluoride/titanium dioxide solar active photocatalytic membrane with excellent rejection and reduction ability was prepared by phase inversion technique. The ex situ formed titanium dioxide nanoparticles using extract of *Cajanus cajan* of average size 10.5 nm were immobilized in the polymer matrix to enhance the performance of polyvinylidene fluoride membrane. This paper explores the innovation of synthesizing a cost-effective bifunctional membrane to eliminate toxic heavy metal: hexavalent chromium from wastewater using a synergistic approach of separation to reject hexavalent chromium and further reducing the toxicity by photocatalytic reduction of concentrated hexavalent chromium. The purpose of this work is to optimize the process condition that governs the process, namely pH, transmembrane pressure (Pa) and chromium concentration (mg/l), to maximize the rejection and reduction percentage using the same material. A quite high value of 97.59% rejection and 91.733% reduction values were suggested by response surface methodology at the predicted value of parameters: pH 5.55, 3.608×10^5 Pa and at 26.652 mg/l. Real industry was also treated and could achieve > 90% rejection and > 85% reduction of Cr.

Keywords Inversion · Nanoparticle · Reduction · Rejection

Introduction

Chromium, a highly toxic heavy metal, exists in two forms as trivalent (Cr(III)) and hexavalent (Cr(VI)). The property of Cr(VI), including non-biodegradability, carcinogenicity and highly corrosive nature, is considered environmentally more hazardous compared to trivalent chromium not only to human life but also to flora and fauna (Jyothi et al. 2017). Hexavalent chromium is considered as one of the top twenty significant contaminants in the priority list of hazardous substances. The potential sources for Cr(VI) discharge to water are leather tanning, metal finishing, electroplating, etc. (Zhang et al. 2020); thus, the government and organization are forcing restriction and applying strict regulation on industries to limit their discharges. US Environmental Protection Agency (USEPA) sets 100 µg/l as the maximum contamination level (MCL) for total Cr in drinking water, whereas World Health Organization (WHO) recommends a maximum allowable concentration of 50 µg/l (Jyothi et al. 2017). So it becomes crucially important to control the high level of carcinogenic and toxic Cr(VI) released from different industries to meet the water quality according to the permissible standard. In the last many years, the use of various technologies for the elimination of Cr(VI) like adsorption, ion exchange and electrochemical reduction had significant drawbacks. The drawback of conventional techniques (adsorption, chemical precipitation, coagulation) includes ineffective removal of metal at low concentration, increased volume of sludge generation and difficulty in their disposal (secondary pollutant generation), and requires high chemical consumption, relatively high operational cost, nondestructive process and incompatibility for large-scale application (Crini and Lichtfouse 2019; Burakov et al. 2018).

In contrast, the emergent technologies like ion exchange, electrodialysis, reverse osmosis and photocatalyst have effective removal capacity as well as low-volume sludge production, but they are expensive, and their reusability is difficult and hence adds additional cost for their recovery (Barakat and Schmidt 2010); also poor recovery of direct use

Editorial responsibility: M. Abbaspour.

✉ Z. Arif
zeenata.rs.che15@itbhu.ac.in

[1] Department of Chemical Engineering and Technology, IIT (BHU) Varanasi, Varanasi, UP, India

of photocatalytic material limits its successful application in suspended form (Jyothi et al. 2017). In comparison with the above-mentioned technique, photocatalytic membrane technology is a one-step treatment procedure that includes the synergistic effect of both organic and inorganic materials, does not require chemical consumption, removes the toxic metal from wastewater and retreats the feed wastage (retentate) using the same membrane as photocatalyst. Immobilization of these high-demand materials on polymer matrix called polymer composite leads to a uniform distribution of particles along with the formation of reactive surfaces with enhanced purification process (Ramasundaram et al. 2016). This synergistic effect will enhance the reusability of material and eliminates the generation of a secondary pollutant.

Membrane separation processes using polymer composite being inexpensive with excellent stability at extreme pH conditions had been the attraction of the present research. Among the various pressure-driven processes, ultrafiltration (UF) proves to be a promising technology than nanofiltration (NF) and reverse osmosis (RO) because of good energy saver with higher flux (Choudhury et al. 2018). Polyvinylidene fluoride (PVDF) has wide commercial availability for UF applications due to outstanding resistivity to organic and inorganic acids (Arif et al. 2019a, b). However, high hydrophobicity of PVDF adversely affects the performance of the membrane. Techniques like graft polymerization, chemical grafting and physical blending had been adopted to tune the hydrophobicity to hydrophilicity, but weak interaction between host matrix and filler diminishes the life span of composite material (Arif et al. 2019a, b). Immobilization of inorganic particles (photocatalyst) into polymer matrix overcomes the disadvantage of using suspended particles and, at the same time, significantly enhances the flux and improves the self-cleaning property. Among different types of existing nanoparticles (NPs) (Ramasundaram et al. 2016; Sharma et al. 2017; Mittal et al. 2015; Choi et al. 2006), nanosized titanium dioxide (TiO_2) is widely used because of easy process ability and superhydrophilicity and imparts catalytic property.

The novelty of this study is using first-time titanium dioxide nanoparticle derived from low-cost and environmentally friendly materials (extract of *Cajanus cajan* which can be easily obtained from kitchen waste, thus reducing the chemical consumption) as filler to the polymeric membranes and inducing excellent properties to separate and reduce the toxic hexavalent chromium to non-toxic trivalent chromium from wastewater. The presence of active substance (terpenoids, aliphatic and aromatic amines) in extract helps in efficient stabilization and prevents agglomeration of NPs. The present study focuses on the application of TiO_2 NPs of different loadings synthesized by green route using an extract of *C. cajan* embedded in PVDF polymer to develop a photocatalytic membrane. It is a well-known fact that feed wastage in the membrane process in the form of retentate remains at the end of the filtration process, and Cr(III) is very less toxic compared to Cr(VI). Thus, the main objective of this study aims to reject and reduce the toxic metal Cr(VI) from water, thus preventing the waste production, minimizing the feed wastage and simultaneously reducing the human capital by using same material (PVDF/TiO_2) firstly as membrane to reject Cr(VI) from wastewater and then as photocatalytic material to reduce the concentrated Cr(VI) to non-toxic Cr(III) from without compromising its efficiency. Till now, very rare literature is available on the application of bifunctional photocatalytic membrane and its optimization for the rejection and reduction of Cr(VI) species using response surface methodology (RSM), and also, the RSM model is very rarely applied for the synthesized membrane. At the same time, the existing conventional analyses are time-consuming and rigorous, and % error is high because they ignore the interaction effects and quadratic effects of dependent factors (Dixit and Yadav 2019). But in real application, these quadratic and interaction effects are important as they govern the accurate optimization for maximizing the desired response. This paper aims to conduct and formulate mathematical predictive models for the approximation to optimize the governing process condition (pH, transmembrane pressure, Cr concentration) using the response surface methodology (RSM) tool to analyze its outcome on the response (% rejection and % reduction). This methodology reduces the number of experiments and optimizes the parameter to achieve maximum rejection and reduction using same material, which has still not been reported. The statistical technique was also employed to obtain the optimum process condition with remarkable improvement in % rejection and % reduction. After optimization, green synthesized photocatalytic membrane at the suggested optimized condition was further used to treat real industry wastewater high in Cr concentration to further validate the applicability of the developed membrane, which has not been published yet.

All the experiments and modeling were performed in the Research Lab of Department of Chemical Engineering technology, IIT (BHU) Varanasi, during month November 2019.

Materials and methods

Material

Base polymer polyvinylidene fluoride (PVDF) (average molecular weight $M_w = 534{,}000$ g/mol) and organic solvent *n*-methyl-2-pyrrolidone (NMP) were purchased from Sigma-Aldrich (Bombay, India). Titanium isopropoxide (TTIP) ($Ti[OCH(CH_3)_2]_4$), a precursor for TiO_2 synthesis, potassium dichromate and diphenylcarbazide were purchased from Merck (Bombay). Double-distilled water (DD) prepared in the laboratory was used in all experiments.

Green synthesis TiO_2 nanoparticles (NPs) using extract *C. cajan*

Split and dehusked arhar pulse (dal) (botanical name *C. cajan* seeds), which can be easily found in kitchens, were thoroughly washed several times to remove surface dust. 15 g of cleaned pulse seeds was soaked in 40 ml distilled water in a beaker and heated to 75 °C for 4 h. Afterward, the extract was filtered through a Whatman No. 01 filter paper, and the collected filtrate was used for the synthesis of TiO_2 nanoparticles. TTIP solution (5 mM, 45 ml) as a precursor was mixed to 15 ml of pulse extract in the ratio of 3:1 (v/v) followed by continuous stirring at ambient temperature for 7 h. High-speed research centrifuge—TC 4100 F—at 9000 rpm for 20 min was used to separate the powder from the extract. The obtained very light yellow color powders were dried at 80 °C overnight and further calcined at 570 °C in a muffle furnace for 2.5 h to remove any organic impurity left to obtain a white color powder.

Preparation of PVDF/TiO_2 composite membranes

Firstly the PVDF pellets and TiO_2 NPs were kept in an oven maintained at 90 °C for 4 h to remove moisture. A dried PVDF pellet (30 g) was added to NMP solvent (140 ml), and the solution was stirred at 70 °C for 0.5 h to achieve a homogeneous solution. In the meantime, a suspension of TiO_2 and NMP was prepared in a beaker and sonicated for 0.5 h. After 0.5 h, TiO_2 suspension was mixed to the prepared polymeric solution and again stirred for 8 h at 70 °C. The prepared casting solution was cast as a film on a glass plate, maintaining a clearance of 160 µm, and then placed in a water bath at temperature (28 ± 1 °C) for 24 h for immersion precipitation. The membranes were then peeled off, washed and stored underwater for further analysis.

Characterization

Morphology of the particle was studied using high-resolution transmission electron microscope (HRTEM), model: Tecnai G2 20 TWIN of USA (SEA), PTE, Ltd, and elemental analysis was carried out using energy-dispersive X-ray spectroscopy (EDAX). Particle synthesis was confirmed using SmartLab X-ray diffractometer (Rigaku SmartLab powder type, without χ-cradle) and also ensured the incorporation of a particle within the polymer matrix. It is a rotating anode XRD operated at 18 KW and consists of CuKα radiation of λ 1.5406 nm. The morphological changes before and after Cr removal were studied Fourier transform spectroscopy (FTIR) of Thermo Nicolet, whereas the surface area of the film was analyzed using BET (model BELLSORP MAX II and BELCAT-II)

Experimental design and modeling using RSM

A statistical method, response surface methodology (RSM), is used here that includes the interaction effects between the considered factors, which were ignored in conventional methods. It is most widely used nowadays to optimize and analyze the response of interest as it reduces the number of experiment without affecting the interactive parameter (Goyal et al. 2011). In the literature, there is not much information available on RSM optimization of Cr rejection and reduction using a bifunctional membrane simultaneously. In this study, a standard RSM design called central composite design (CCD) was employed to test the influence of independent variables (pH, membrane pressure, chromium concentration) on the dependent variable: rejection and reduction of chromium from an aqueous solution. The condition ranges of the above influencing parameter are pH 5–8, pressure $1–4 \times 10^5$ Pa and Cr concentration 25–50 mg/l. These three process variables were rigorously examined and were optimized using the RSM of Design Expert 8.0 software. The main goal, i.e., the maximum value of rejection and reduction, will determine the optimized values of the process variable and will indicate the performance of the TiO_2-enhanced PVDF polymer ultrafiltration process. The design comprised of 20 experimental trials including six center points to maintain the accuracy. The number of experiments was determined using Eq. 1 (Tan et al. 2008)

$$M = 2^m + 2m + m_c \tag{1}$$

where m represents the number of independent variable as 3 and m_c represents the number of replicate as 6; thus, the calculated number of experiment (M) is 20 and is shown in Table 1

To optimize the independent variables for the responses (% rejection and % reduction) obtained from experiments, the second-order polynomial equation incorporating quadratic and interaction term was applied from the CCD model. Generalized mathematical form to represent the second-order equation is shown in Eq. (2).

$$R_y = \alpha_o + \sum_{i=1}^{m} \alpha_i X_i + \sum_{i=1}^{m} \alpha_{ii} X_i^2 + \sum_{i<j}^{m} \alpha_{ij} X_i X_j \tag{2}$$

where R_y denotes response, X_i and X_j are the coded values, α_o, α_i, α_{ii} and α_{ij} are the regression linear, quadratic and interaction coefficients, respectively, and m is a number of the design process variable. A statistical tool, analysis of variance (ANOVA), was employed to validate the reliability of the equation generated using RSM. The statistical fitness of the CCD model was examined using different factors of ANOVA that include determination coefficient (R^2), adjusted determination of coefficient (R^2_{adj}), F value, p value and degree of freedom (df).

Table 1 CCD experimental design of experimental matrix for Cr(VI) removal by PVDF/TiO_2 membrane

Runs	pH	Pressure × 10^5 (Pa)	Concentration (mg/l)	Rejection (%)	Reduction (%)
1	5	1	25	92.74	90.89
2	8	1	25	75.02	71.98
3	5	4	25	94.98	89.07
4	8	4	25	78.9	72.84
5	5	1	50	85.01	80.012
6	8	1	50	69.08	63.01
7	5	4	50	89.21	79.9
8	8	4	50	72.28	62.9
9	5	2.5	37.5	90.28	88.9
10	8	2.5	37.5	73.91	69.98
11	6.5	1	37.5	91.5	89.03
12	6.5	4	37.5	93.01	87.8
13	6.5	2.5	25	94	88.9
14	6.5	2.5	50	92.2	80
15	6.5	2.5	37.5	93.98	88.75
16	6.5	2.5	37.5	93.98	88.75
17	6.5	2.5	37.5	93.98	88.75
18	6.5	2.5	37.5	93.98	88.75
19	6.5	2.5	37.5	93.98	88.75
20	6.5	2.5	37.5	93.98	88.75

Performance analysis

Based on the optimum value as suggested by RSM, an experiment was performed at the given condition using an ultrafiltration setup. It consists of flow filtration cell of filtration area of 15 m^2. Initially, the membrane was pre-pressurized for half an hour at given pressure to achieve stable flux. Then a 500 ml chromium solution at the suggested concentration and pH value was passed through the membrane. Chromium concentration in retentate and permeate was estimated from the standard calibration curve (absorbance v/s concentration of Cr(VI)) obtained by adding a 1,5 diphenylcarbazide to Cr solution to give absorbance value at wavelength 540 nm using a spectrophotometer (SYSTRONICS, PC Based Double Beam Spectrometer 2202). The retentate rich in the concentrated chromium was further subjected to photocatalytic reduction under sunlight. The retentate sample was poured into the beaker consisting of the used washed membrane fixed at the bottom. 10 ml samples was collected at regular intervals and analyzed for Cr(VI).

The reusability of the product is also one of the vital parameters for the successful application at massive scale. The reusability test was carried out by running the experiments five times by maintaining the same operating condition and used membrane material. After each run, membrane sample was washed with Millipore water to remove residual from it and is again reused following the above-described method. The membrane before and after experiment was also analyzed under FTIR and BET to study the morphological changes.

Performance of membrane in real wastewater

At the suggested optimum condition, the developed photocatalytic membrane was subjected to treat real wastewater using the same procedure as done for a model solution. Wastewater sample was collected from three different types of tannery industries located in an industrial area, Site-2 Unnao, UP. The area is very well famous for leather manufacturing and its export. The chromium concentration was measured using inductively coupled plasma mass spectrometry (ICP-MS) of Agilent 7800 ICP-MS mainframe, Agilent Technologies, and chemical oxygen demand (COD) was evaluated using a COD digester (UNIPHOS)

Results and discussion

Morphology of NPs

The morphology of synthesized particle was analyzed using HRTEM, as shown in Fig. 1a, b. The image reveals mostly spherical shape particle in size ranges from 9 to 14 nm with an average size of around 10.5 nm. Observation made from the SAED pattern, as shown in Fig. 1b, confirms polycrystalline anatase structure (Kalaiarasi et al. 2018). The elemental analysis was studied using EDAX image shown in Fig. 1c. Sharp peaks of only O and Ti signify the formation of TiO_2 NPs.

XRD pattern of synthesized NPs and membranes is shown in Fig. 1d. The existence of significant peak obtained at 2 θ 25.5°, 37.9°, 48.3°, 53.4°, 55.3° and 62.2° is in accordance with JCPDS card, 21-1272; hence, it confirms the formation of anatase phase TiO_2 nanoparticles (Kumar et al. 2019). In case of PVDF and PVDF/TiO_2 membrane, the existence of a strong peak corresponding to 2θ at 20.4° depicts β-phase of PVDF, and the existence of six additional peaks ensures that particles are well embedded within the polymer matrix as similar peaks were observed in case of pure TiO_2 NPs. It was also observed that the peak intensity at $2\theta = 20.4°$ is small compared to pure PVDF membrane due to the presence of TiO_2, thus moving toward an amorphous region and beneficial for membrane application (Arif et al. 2019a, b; Meng et al. 2016).

Mechanism for Cr(VI) removal from wastewater using bifunctional membrane

It was reported in the literature that Cr(VI) ions exist in $Cr_2O_7^{2-}$, CrO_4^{2-} and $HCrO^{4-}$ form in an aqueous solution at acidic pH (Kazemi et al. 2018) and the amphoteric nature of TiO_2 particle due to protonation and deprotonation of

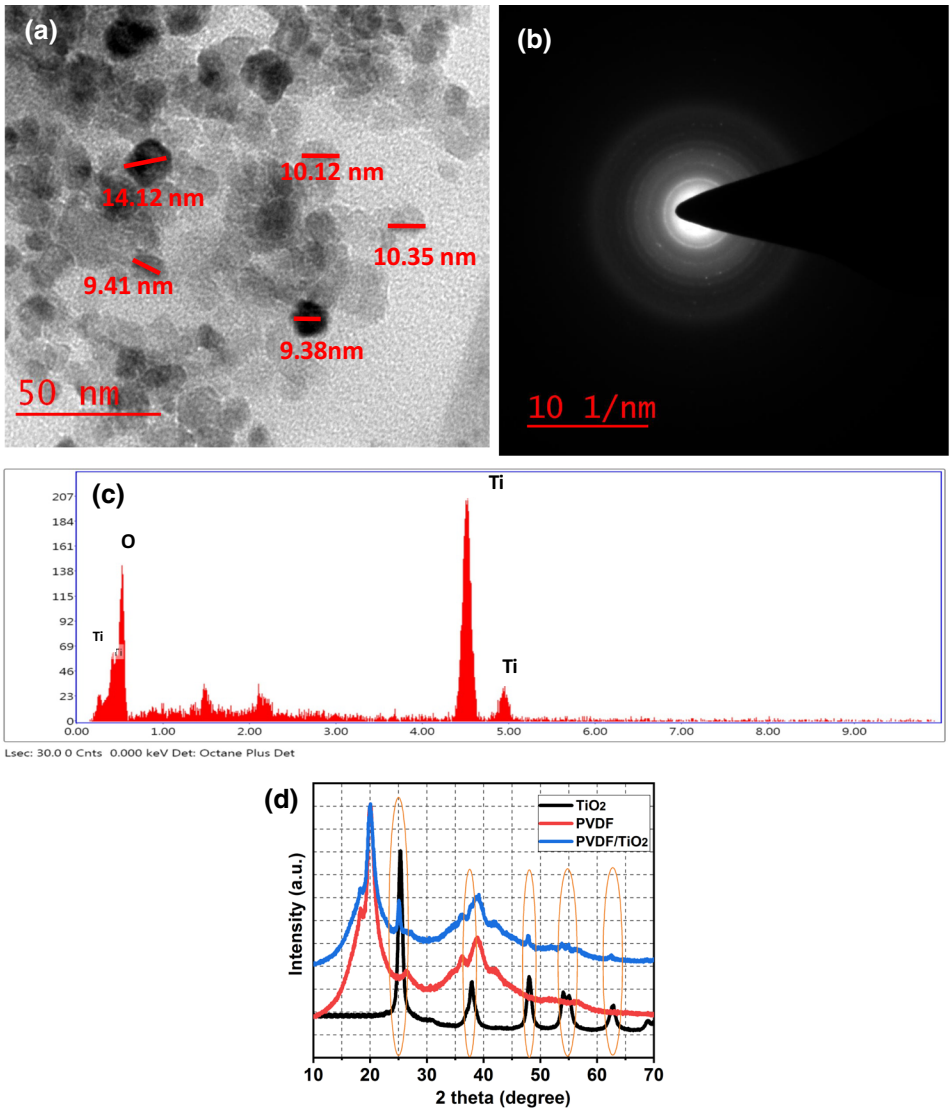

Fig. 1 **a** TEM image, **b** SAED pattern, **c** EDAX of TiO_2 nanoparticle and **d** XRD pattern of synthesized TiO_2 NPs, PVDF and PVDF/TiO_2 composite membrane

hydroxyl groups on the surface exists in Ti–OH_2^+ in acidic environment as shown in Eq. (3)

$$(\text{Ti}-\text{OH})_{\text{surface}} + H_3O^+ \leftrightarrow \text{Ti}-OH_2^+ + H_2O \quad (3)$$

Thus, TiO_2 particle can adsorb the mentioned anions ($Cr_2O_7^{2-}$, $CrO_4^{2-}$and $HCrO^{4-}$) due to the presence of Ti–OH_2^+. Thus, it is the electrostatic interaction that is responsible for the rejection of Cr(VI) from wastewater when using TiO_2/PVDF membrane material during ultrafiltration. With the same material when used as photocatalytic film to reduce the concentrated Cr(VI) and collected at retentate; it was predicted that under sunlight photons emitted were adsorbed by TiO_2 and produce e^{-CB} and h^{+VB} as shown in Fig. 2 and Eqs. (4–6) which is the reason for reducing Cr(VI) to Cr(III) form

$$TiO_2 + hn \rightarrow e^{-CB} + h^{+VB} \quad (4)$$

$$Cr_2O_7^{2-} + 14H^+ + 6e^{-CB} \rightarrow 2Cr^{3+} + 7H_2O \quad (5)$$

$$2H_2O + 4h^{+VB} \rightarrow O_2 + 4H^+ \quad (6)$$

RSM and ANOVA

Data adequacy check of the model

A set of experiments as suggested by RSM were performed, and the experimentally obtained data were analyzed using ANOVA. Figure 3 depicts the actual versus predicted responses (% rejection and % reduction).

Here, the actual values were determined experimentally, and predicted values were calculated and provided by the RSM model. Figure 3a plot indicates that the model is adequate and ensures the acceptability of the predicted model because almost

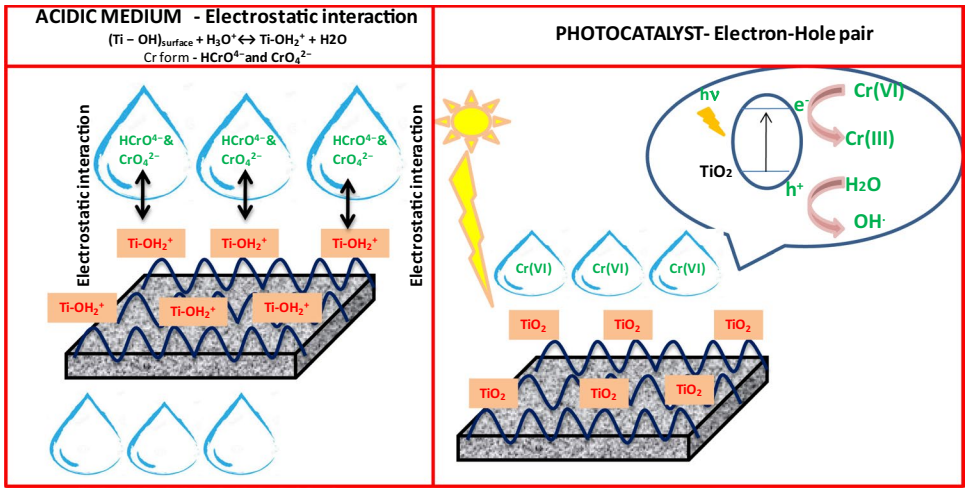

Fig. 2 Schematic representation of the mechanism from Cr(VI) removal

all the points in both the plots lie on the diagonal line, and if not, they are close very close to the diagonal line (Lu et al. 2009). Model reliability was further assured in terms of R^2. Here, the high value of R^2 and adjusted R^2 > predicted R^2 in case of % rejection is 0.9812 > 0.9216, and for % reduction, it is 0.9958 > 0.9767 which confirms that results fit well with the predicted value. The normal distribution of internally studentized residuals is shown in Fig. 3b for the process response. The plot depicts a high degree of fitness due to a linear profile with a minimal variation in the variance, hence assuring that the error terms were distributed normally for the process response.

Effect of independent (process) variables on % rejection

Quadratic order has been suggested for regression analysis without any transformation, and the RSM equation in terms of actual factor is shown in Eq. 7

$$\begin{aligned}\%\ \text{Rejection} = {} & +93.59 - 8.30\ \text{pH} + 1.50\ \text{pressure} \\ & - 2.79\ \text{concentration} \\ & + 0.0800\,(\text{pH} * \text{pressure}) \\ & + 0.1175\,(\text{pH} * \text{concentration}) \\ & + 0.1600\,(\text{pressure} * \text{concentration}) \\ & - 10.92\,(\text{pH})^2 - 0.7568\,(\text{pressure})^2 \\ & + 0.0882\,(\text{concentration})^2 \end{aligned} \quad (7)$$

The fitted model includes each contributing factor for a response. The adequacy of the second-order equation was analyzed using Fisher's statistical test (F value) defined as a ratio of mean $\text{square}_{\text{regression}}$ to the mean $\text{square}_{\text{residual or real error}}$. The suitability of the model is well defined as a probability value (p value) is < 0.05 with high F value. Value of $p < 0.0001$ and 111.35 as F value in Table 2 implies that the model is statistically significant and well suited to the experiments. It is not necessary to have all terms significant in regression analysis. If p values of regression are less than 0.0500, it is affirmed that terms are significant, and here, linear terms, namely pH, pressure, concentration, and quadratic term pH^2, are significant model terms. Moreover, the model significance was further reinforced by the "Adeq precision" ratio, which was found to be 32.147, which indicates an adequate signal as a ratio above 4 is desirable and hence can be effectively used to navigate design space.

The developed regression equation generates graphical response surfaces. This response plot helps in determining the individual and combined effects of an independent variable. Based on ANOVA for this study, it was observed that pH is a more significant parameter than concentration and lastly pressure on % rejection of Cr(VI). Figure 4 shows the 3D plot of response as a function of independent variables. Figure 4a–d depicts lesser % rejection at high pH value; a similar results were also mentioned in the literature (Gasemloo et al. 2019; Zhang et al. 2020), because at low pH value Cr(VI) exists in anionic form ($HCrO_4^-$) and positive charge was induced on the membrane surface due to the presence of TiO_2 NPs; as a result, strong electrostatic interaction leads to increased Cr removal. This implies significant impact of pH on % rejection. Trend similar to pH was observed on increasing the Cr(VI) at constant pH as shown in Fig. 4c–f. The increased concentration at acidic pH generates an excess anionic charge on the membrane surface and thus creates a negative impact on membrane separation efficiency. The effect of transmembrane pressure is less significant compared to other independent variables, as shown in Fig. 4a, b, e, f. The small increase in % rejection was observed on increasing the pressure due to an increase in solvent convective transport; similar trend was also reported by Riaz et al. (2016). These results conclude that there is considerable interaction of independent parameters for optimization of % rejection and also highlights that pH is an eminent factor affecting the membrane performance.

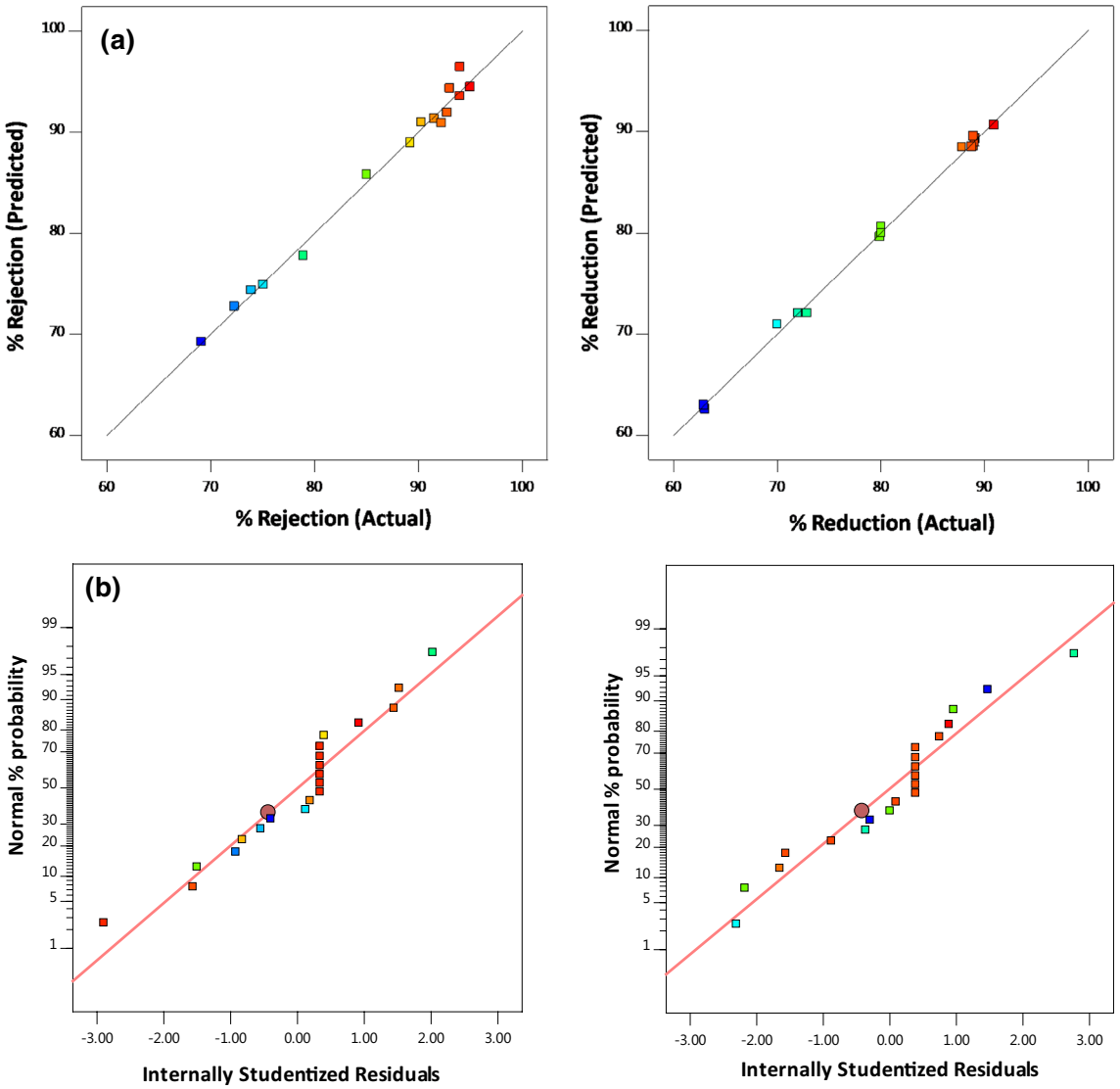

Fig. 3 Diagnostic plots **a** actual versus predicted plot of model and **b** internally studentized plots

Effect of independent (process) variables on % reduction

The statistical equation obtained for reduction using RSM is shown in Eq. 8

$$\begin{aligned}\%\ \text{Rejection} = {} & +88.53 - 8.81 * \text{pH} - 0.2412 * \text{pressure} \\ & - 4.79 * \text{concentration} \\ & + 0.3352\,(\text{pH} * \text{pressure}) \\ & + 0.1422\,(\text{pH} * \text{concentration}) \\ & + 0.0923\,(\text{pressure} * \text{concentration}) \\ & - 8.76\,(\text{pH})^2 - 0.2178\,(\text{pressure})^2 \\ & - 3.75\,(\text{concentration})^2 \end{aligned} \quad (8)$$

Herein, also p value < 0.0001 and 505.70 of F value (Table 3) from ANOVA affirms that the model is significant. It was also observed that p value is < 0.05 for linear term (pH and concentration) and quadratic term (pH^2 and concentration^2) signifies remarkable impact of these independent variables on % reduction.

Response 3D plots for % reduction showing the interaction between independent and dependent variables are shown in Fig. 5. Images in Fig. 5a–d depict that pH plays a crucial role during photocatalytic process; this is due to the fact that variation in pH will directly influence surface charge directly affecting the photoreduction process (Mohamed et al. 2016). A trend similar to % rejection was obtained here also, which implies that % reduction will be higher at acidic pH; Fig. 5c–f shows the effect of Cr concentration on % reduction. It was concluded that with an

Table 2 ANOVA summary for % rejection from CCD model

Source	Sum of squares	*df*	Mean square	*F* value	*p* value	
Model	1432.16	9	159.13	111.35	< 0.0001	Significant
pH	689.40	1	689.40	482.41	< 0.0001	
Pressure	22.59	1	22.59	15.81	0.0026	
concentration	77.62	1	77.62	54.31	< 0.0001	
pH*pressure	0.0512	1	0.0512	0.0358	0.8537	
pH*concentration	0.1105	1	0.1105	0.0773	0.7867	
Pressure*concentration	0.2048	1	0.2048	0.1433	0.7129	
pH^2	327.74	1	327.74	229.34	< 0.0001	
$Pressure^2$	1.58	1	1.58	1.10	0.3185	
$Concentration^2$	0.0214	1	0.0214	0.0150	0.9051	
Residual	14.29	10	1.43			
Lack of fit	14.29	5	2.86			
Pure error	0.0000	5	0.0000			
Cor total	1446.45	19				
SD	1.20	R^2	0.9901			
Mean	87.80	Adjusted R^2	0.9812			
C.V.%	1.36	Predicted R^2	0.9216			

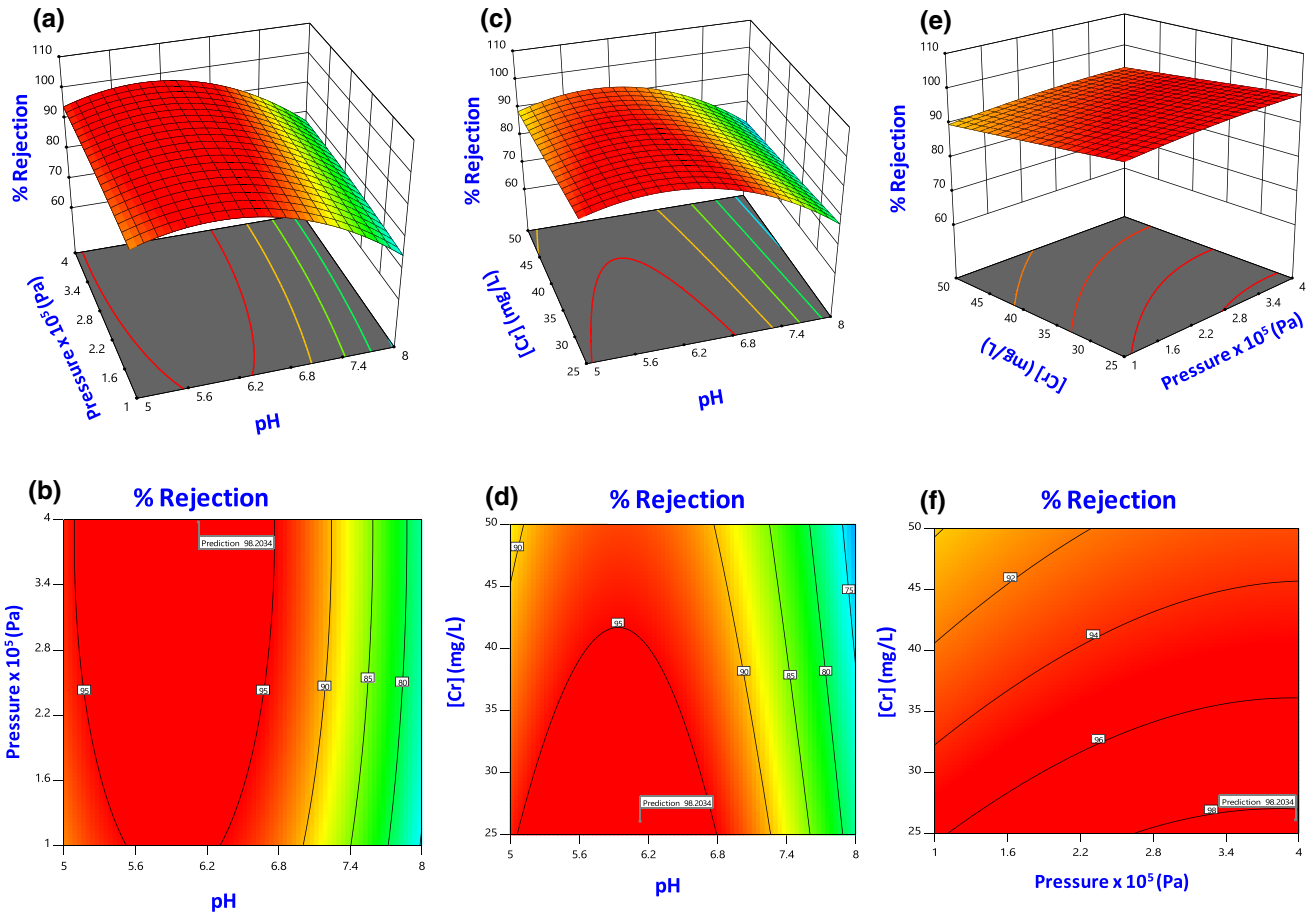

Fig. 4 3D response surface and contour plots of % rejection showing the effect of **a**, **b** pH and pressure; **c**, **d** pH and concentration; **e**, **f** concentration and pressure

Table 3 ANOVA for % reduction from CCD model

Source	Sum of squares	*df*	Mean square	*F* value	*p* value	
Model	1640.67	9	182.30	505.70	< 0.0001	Significant
pH	775.49	1	775.49	2151.26	< 0.0001	
Pressure	0.5818	1	0.5818	1.61	0.2327	
concentration	229.04	1	229.04	635.37	< 0.0001	
pH*pressure	0.8991	1	0.8991	2.49	0.1453	
pH*concentration	0.1619	1	0.1619	0.4491	0.5180	
Pressure*concentration	0.0681	1	0.0681	0.1889	0.6731	
pH^2	210.89	1	210.89	585.03	< 0.0001	
$Pressure^2$	0.1305	1	0.1305	0.3619	0.5608	
$Concentration^2$	38.61	1	38.61	107.12	< 0.0001	
Residual	3.60	10	0.3605			
Lack of fit	3.60	5	0.7210			
Pure error	0.0000	5	0.0000			
Cor total	1644.28	19				
SD	0.6004	R^2	0.9978			
Mean	82.39	Adjusted R^2	0.9958			
C.V.%	0.7288	Predicted R^2	0.9767			

increase in concentration at constant pH photoreduction efficiency decreases. This is attributed to the fact that increased concentration will interfere with the light reaching the photocatalytic surface due to increased absorbance capacity at high concentration, thereby reducing the degree of reduction (Qamar et al. 2011). The third independent variable (pressure) is not a significant parameter in this case; as shown in Fig. 5a, b, e, f, no significant change is observed with the change in pressure.

Hence, it can be concluded that pH and concentration significantly affect both two responses (% rejection and % reduction), while transmembrane pressure is effective for % rejection only. Percentage effect of each contributing factor (Fig. 6a) on the two responses will be estimated using a Pareto chart (Gasemloo et al. 2019) and is expressed as shown in Eq. 9

$$P_j = \left(\frac{\beta_j^2}{\sum \beta_j^2} \right) \times 100 \quad \text{where } j \neq 1 \tag{9}$$

Here, P_j refers to the percentage effect of factor and β_j represents the coefficient of each factor

Optimization and validation of optimized results

After the establishment of the quadratic equation relating the dependent variable with the independent variable, it is checked further for optimization. The main objective of experimental designing and optimization is to determine the optimum values of the parameter at which maxima or minima of response output could be achieved. In this study, the desired goal for the two responses is set as "maximum," while for process variable, the desired goal was marked as "range." The optimum result obtained from numerical optimization from CCD model is shown in Fig. 6b. Under the given the suggested optimum condition, an experiment was performed to verify and validate the result. The experimental result obtained was consistent with the results obtained from RSM and hence validated the findings of response surface optimization, and the percentage error is almost negligible.

Reusability and stability

The potential of any product relies on the reusability of the material without compromising the efficiency. At the given optimized condition to test the reusability of PVDF/TiO_2 membrane, the experiment was run six times, and the result is shown in Fig. 6c. No significant loss could be observed which implies that synthesized PVDF/TiO_2 membrane retains its reusable capacity.

Also, Fig. 6d shows FTIR spectra of the composite membrane at different conditions during the experiment. It was observed that peaks obtained for cleaned membrane after separation and photocatalytic application were similar to the fresh membrane (original membrane). Peaks at wavelength 3748 and 1658 correspond to the hydroxyl group from TiO_2, and peak at 640 cm^{-1} corresponds to Ti–O–Ti bonds (Bhute et al. 2017). It signifies no morphological changes were observed; hence, membrane retains its property even after using it as membrane and photocatalytic film. After completion of the separation process, peaks are either diminish or vanished, which signifies that these peaks play a great role for separation because, as already mentioned it is the ionic interaction responsible for the separation of

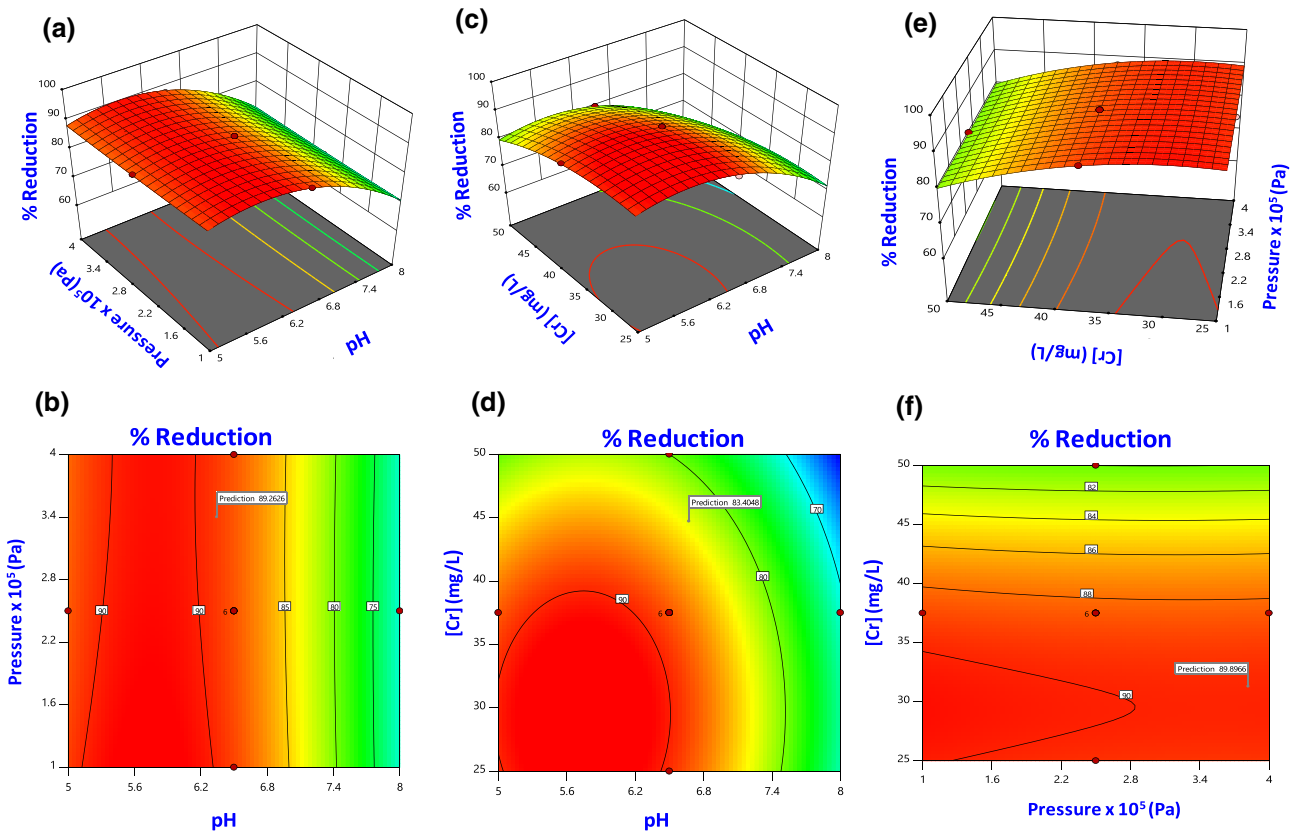

Fig. 5 3D response surface and contour plots of % reduction showing the effect of **a**, **b** pH and pressure; **c**, **d** pH and concentration; **e**, **f** concentration and pressure

Cr(VI) from wastewater. The results were justified from BET (Brunauer, Emmett and Teller) analysis of composite film before and after Cr removal, as shown in Fig. 6e. The estimated BET surface area before and after Cr removal using the BET equation was 383.5 and 366.7 m^2/g (Judai et al. 2015), respectively. Herein, also not much significant decline in surface area was observed, which implies that PVDF/TiO_2 membrane is having excellent recyclability without much compromising in its efficiency. Particle stability within the polymer matrix is another important point. There may be a possibility that particle may leach out during application and can affect the hydrophilicity. The measurement of the contact angle to ensure the hydrophilicity of the membrane acts as a stability indicator (Arif et al. 2019a, b). Figure 6f depicts the contact angle of the cleaned membrane after Cr removal. It was concluded from here that no drastic difference in value was observed, which proves excellent stability of synthesized TiO_2 NPs within the PVDF polymer.

Lastly, the performance of the synthesized membrane was checked using real tannery wastewater. The results obtained are shown in Fig. 6g.

Figure 6g depicts that approximately 90% rejection and 89% reduction of Cr could be achieved for three different types of the leather industry, which is comparable to results obtained using the model chromium solution. Thus, it can be said that green synthesized TiO_2 nanoparticle embedded in PVDF polymer provides can be used to treat wastewater in a cost-effective way using the ultrafiltration process. A comparative study is also carried to compare the efficiency reported in this work with other published literature, as shown in Table 4. It was concluded from the figure that either expensive technique is required to treat real wastewater to achieve rejection > 90%, or in other cases, if separation efficiency is > 90%, it is only reported for model Cr solution. However, in this study, both separation efficiency and % reduction are above > 90% applicable for both model and real solutions using cost-effective ultrafiltration process.

Effect of coexisting ions on Cr removal

To address and understand the role of electrostatic interaction affecting the Cr(VI) removal, the presence of other metal mono- and bivalent ion (Na^+, Pb^{2+}) interfering process was also investigated. Each concentration of ion was measured using inductively coupled plasma (ICP) instrument.

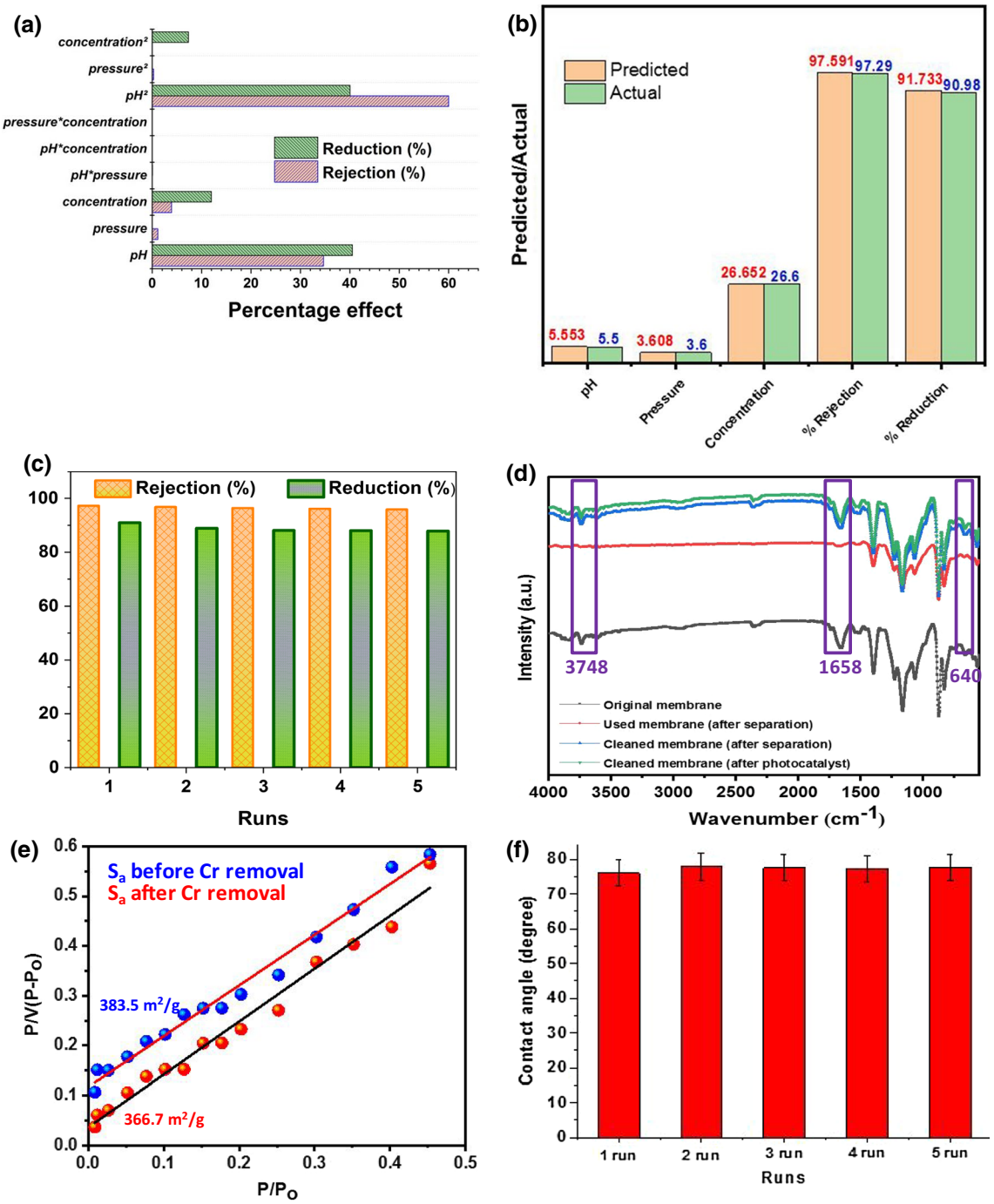

Fig. 6 **a** Pareto chart for Cr(VI) removal from wastewater, **b** predicted and experimental (actual) value at optimized condition, **c** reusability of PVDF/TiO_2 membrane for Cr(VI) removal (**d**), FTIR spectra of membrane at different operating conditions (**e**), BET before and after Cr removal (**f**), **g** graph of pH, TSS, COD and Cr for wastewater before and after treatment for three different types of tannery industry

Since the aim of this paper on Cr(VI) removal, the results will be represented for diffused Cr ion removal in the permeate side at a given optimized condition. Figure 7 shows the % rejection profile of Cr(VI) in the presence of other metal ions. It was concluded that % rejection of Cr (approx 96%) reflects a negligible change in value in the presence of Na^+ ion; however, that is not the case with the bivalent ion. Rejection of approx. 90% was observed in the presence of Pb^{2+} ion. The present result very well correlates with other published literature (Zhang et al. 2020). This effect is because the rejection is dependent on the ion mobility and also the number of ionic pairs formed between membranes

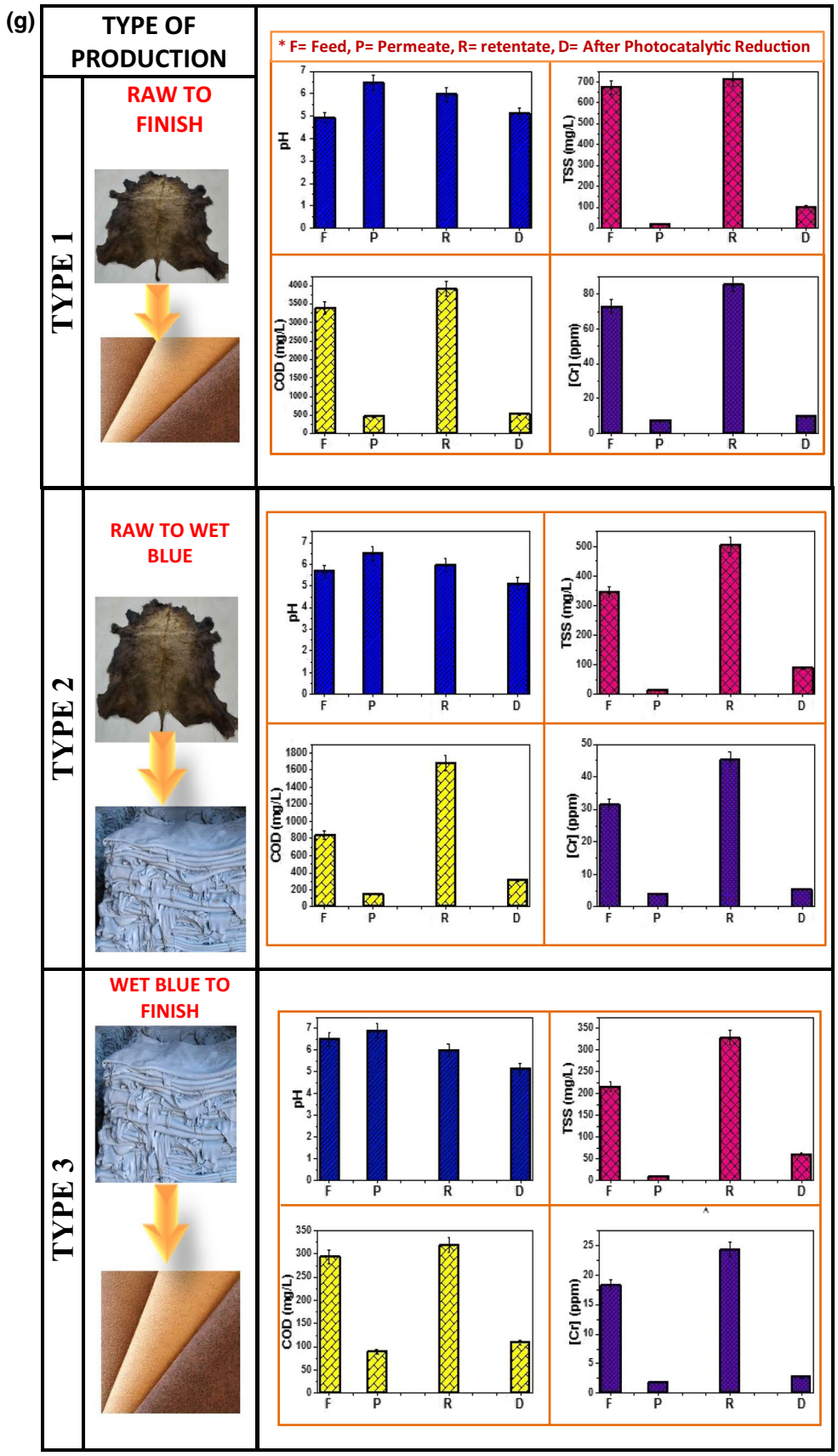

Fig. 6 (continued)

Table 4 Comparative study of the present study with other published literature

Process	Synthesis/commercial	% Removal	References
Anaerobic nano zero-valent iron granules	Synthesized	Model Cr solution 88 ± 1.56% rejection	Venkata Giri et al. (2019)
Membrane bioreactor and reverse osmosis treatment	Synthesized	Real wastewater 97% rejection	Scholz et al. (2005)
Nanofiltration membrane	Synthesized	Real wastewater 60–80% rejection	Mohammed and Sahu (2019)
Conductive ultrafiltration	Synthesized	Model Cr solution 72.4% rejection	Liu et al. (2019)
Amine-impregnated TiO_2 nanoparticles modified cellulose acetate membranes	Synthesized	Model Cr solution 72.4% rejection	Alebel Gebru and Das (2018)
Polyamide skin over a polysulfone support—nanofiltration (NF) and polyamide—reverse osmosis (RO)	Commercial	Real wastewater: approx 97% Cr removal	Das et al. (2006)
PVDF/TiO_2 ultrafiltration membrane	Synthesized bifunctional membrane	Model Cr solution 7.2% rejection and 90.98% reduction Real wastewater: > 90% rejection and > 88% reduction	This work

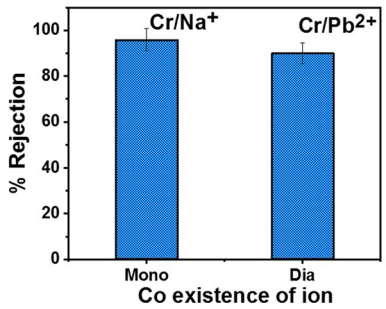

Fig. 7 Percent rejection of Cr in the presence of interfering counterions

due to the presence of the amphoteric nature of particle entrapped within the polymer and contaminant ion. Lesser rejection will be observed at higher charges due to the low mobility of ions (Jyothi et al. 2017). The presence of divalent cation (Pb^{2+}) forms a pair with two fixed charges, thereby decreasing the availability of fixed charges on the membrane, thus leading to the reduced rejection. In the case of monovalent ion, a single fixed charge is consumed; therefore, the value of % rejection is more in this case. These observations signify that the electrostatic attraction between Cr(VI) and PVDF/TiO_2 nanocomposite played a dominant role in rejection.

Conclusion

The present investigation established the low-cost synthesis PVDF/TiO_2 membrane using green synthesized TiO_2 NPs and success of RSM methodology on TiO_2-enhanced PVDF membrane for evaluating the % rejection and % reduction for removal of toxic metal chromium (VI) was discussed. An attempt has been made to apply RSM on bifunctional ultrafiltration membrane which took into consideration the environmental problem pertaining to chromium (VI) removal from an aqueous solutions. The work was done in four steps: Firstly, NPs and films were synthesized and characterized to ensure incorporation of ex situ formed particle using *C. cajan* extract of average size 10.5 nm within the polymer matrix. Secondly, the analysis and optimization of parameter influencing the response of interest using RSM and lastly at optimized condition, results are validated using both model and real wastewater. The CCD model proves to be an effective statistical tool for optimization. The authenticity and accuracy of the predicted model were very well corroborated by the ANOVA, and also the values of R^2 and $R^2_{adj} > 0.95$ imply the reliability of the prediction and refine the model. Results obtained using central composite design (CCD) of RSM indicate that the maximum theoretical values of % rejection and % reduction at optimum condition are 97.59% and 91.733%, respectively, and were well equable with the experimental results under same condition, and for real wastewater, they are approximately 93.8% rejection and 89.57% reduction which implies that low-cost photocatalytic ultrafiltration membrane was successfully developed. It was observed that interaction of pH and concentration is more significant in case of % rejection and % reduction; however, pressure is only significant parameter in case of % rejection.

Acknowledgements The author would like to acknowledge Central Instrument Facility (CIF) IIT (BHU) for XRD, TEM and ICP-MS facility.

Compliance with ethical standards

Conflict of interest The authors declare that they have no conflict of interest in this publication.

References

Alebel Gebru K, Das C (2018) Removal of chromium (VI) ions from aqueous solutions using amine-impregnated TiO_2 nanoparticles modified cellulose acetate membranes. Chemosphere 191:673–684

Arif Z, Sethy NK, Kumari L, Mishra PK, Verma B (2019a) Antifouling behaviour of PVDF/TiO_2 composite membrane: a quantitative and qualitative assessment. Iran Polym J 28:301–312

Arif Z, Sethy NK, Kumari L, Mishra PK, Verma B (2019b) Green synthesis of TiO_2 nanoparticles using *Cajanus cajan* extract and their use in controlling the fouling of ultrafiltration PVDF membranes. Korean J Chem Eng 36(7):1148–1156

Barakat MA, Schmidt E (2010) Polymer-enhanced ultrafiltration process for heavy metals removal from industrial wastewater. Desalination 256:90–93

Bhute MV, Mahant YP, Kondawar SB (2017) Titanium dioxide/poly(vinylidene fluoride) hybrid polymer composite nanofibre as potential separator for lithium ion battery. J Mater Nanosci 4(1):6–12

Burakov AE, Galunin EV, Burakova IV, Kucherova AE, Agarwal S, Tkachev AG et al (2018) Adsorption of heavy metals on conventional and nanostructured materials for wastewater treatment purposes: a review. Ecotoxicol Environ Saf 148:702–712

Choi H, Stathatos E, Dionysiou DD (2006) Sol–gel preparation of mesoporous photocatalytic TiO_2 films and TiO_2/Al_2O_3 composite membranes for environmental applications. Appl Catal B Environ 63:60–67

Choudhury PR, Majumdar S, Sahoo GC, Saha S, Mondal P (2018) High pressure ultrafiltration CuO/hydroxyethyl cellulose composite ceramic membrane for separation of Cr(VI) and Pb(II) from contaminated water. Chem Eng J 336:570–578

Crini G, Lichtfouse E (2019) Advantages and disadvantages of techniques used for wastewater treatment. Environ Chem Lett 17:145–155

Das C, Patel P, De S, DasGupta S (2006) Treatment of tanning effluent using nanofiltration followed by reverse osmosis. Sep Purif Technol 50:291–299

Dixit S, Yadav VL (2019) Optimization of polyethylene/polypropylene/alkali modified wheat straw composites for packaging application using RSM. J Clean Prod 240:118228

Gasemloo S, Khosravi M, Sohrabi MR, Dastmalchi S, Gharbani P (2019) Response surface methodology (RSM) modeling to improve removal of Cr(VI) ions from tannery wastewater using sulfated carboxymethyl cellulose nanofilte. J Clean Prod 208:736–742

Goyal RK, Jayakumar NS, Hashim MA (2011) A comparative study of experimental optimization and response surface optimization of Cr removal by emulsion ionic liquid membrane. J Hazard Mater 195:383–390

Judai K, Iguchi N, Hatakeyama Y (2015) Low-temperature production of genuinely amorphous carbon from highly reactive nanoacetylide precursors. J Chem. https://doi.org/10.1155/2016/7840687

Jyothi MS, Vignesh N, Mahesh P, Balakrishna RG, Soontarapa K (2017) Eco-friendly membrane process and product development for complete elimination of chromium toxicity in wastewater. Hazard Mater 332:112–123

Kalaiarasi S, Sivakumar A, Dhas SAMB, Jose M (2018) Shock wave induced anatase to rutile TiO_2 phase transition using pressure driven shock tube. Mater Lett 219:72–75

Kazemi M, Jahanshahi M, Peyravi M (2018) Hexavalent chromium removal by multilayer membrane assisted by photocatalytic couple nanoparticle from both permeate and retentate. J Hazard Mater 344:12–22

Kumar S, Mishra DK, Sobral AJFN, Koh J (2019) CO_2 adsorption and conversion of epoxides catalyzed by inexpensive and active mesoporous structured mixed-phase (anatase/brookite) TiO_2. J CO2 Util 34:386–394

Liu L, Xu Y, Wang K, Li K, Xu L, Wang J, Wang J (2019) Fabrication of a novel conductive ultrafiltration membrane and its application for electrochemical removal of hexavalent chromium. J Membr Sci 584:191–201

Lu S-Y, Qian J-Q, Wu Z-G, Ye W-D, Wu G-F, Pan Y-B, Zhang K-Y (2009) Application of statistical method to evaluate immobilization variables of trypsin entrapped with sol-gel method. J Biochem Technol 1(3):79–84

Meng N, Priestley RCE, Zhang Y, Wang H, Zhang X (2016) The effect of reduction degree of GO nanosheets on microstructure and performance of PVDF/GO hybrid membranes. J Membr Sci 501:169–178

Mittal A, Naushad A, Sharma G, Alothman ZA, Wabaidur SM, Alam M (2015) Fabrication of MWCNTs/ThO_2 nanocomposite and its adsorption behavior for the removal of Pb(II) metal from aqueous medium. Desalin Water Treat 57:21863–21869

Mohamed A, Osman TA, Toprak MS, Muhammed M, Yilmaz E, Uheida A (2016) Visible light photocatalytic reduction of Cr(VI) by surface modified CNT/titanium dioxide composite nanofibres. J Mol Catal A Chem 424:45–53

Mohammed K, Sahu O (2019) Recovery of chromium from tannery industry waste water by membrane separation technology: health and engineering aspects. Sci Afr 4:e00096

Qamar M, Gondal MA, Yamani ZH (2011) Synthesis of nanostructured NiO and its application in laser-induced photocatalytic reduction of Cr(VI) from water. J Mol Catal A Chem 341:83–88

Ramasundaram S, Seid MG, Choe JW, Kim EJ, Chung YC, Cho K, Lee C, Hong SW (2016) Highly reusable TiO_2 nanoparticle photocatalyst by direct immobilization on steel mesh via PVDF coating, electrospraying, and thermal fixation. Chem Eng J 306:344–351

Riaz T, Ahmad A, Saleemi S, Adrees M, Jamshed F, Hai AM, Jamil T (2016) Synthesis and characterization of polyurethane-cellulose acetate blend membrane for chromium (VI) removal. Carbohydr Polym 153:582–591

Scholz WG, Rougé P, Bódalo A, Leitz U (2005) Desalination of mixed tannery effluent with membrane bioreactor and reverse osmosis treatment. Environ Sci Technol 39(21):8505–8511

Sharma G, Naushad M, Muhtaseb A, Kumar A, Khan R, Kalia S, Bala M, Sharma A (2017) Fabrication and characterization of chitosan-*crosslinked*-poly(alginic acid) nanohydrogel for adsorptive removal of Cr(VI) metal ion from aqueous medium. Int J Biol Macromol 95:484–493

Tan I, Ahmad A, Hameed B (2008) Optimization of preparation conditions for activated carbons from coconut husk using response surface methodology. Chem Eng J 137(3):462–470

Venkata Giri RK, Raju LS, Nancharaiah YV, Pulimi M, Chandrasekaran N, Mukherjee A (2019) Anaerobic nano zero-valent iron granules for hexavalent chromium removal from aqueous solution. Environ Technol Innov 16:100495–100507

Zhang S, Shi Q, Korfiatis G, Christodoulatos C, Wang H, Meng X (2020) Chrmoate removal by electrospun PVA/PEI nanofibres: adsorption, reduction, and effects of co-existing ions. Chem Eng J 387:124179–124188